molecular pharmaceutics

ARTICLE

pubs.acs.org/molecularpharmaceutics

Coformulation of Doxorubicin and Curcumin in Poly-(D,L-lactide-*co*-glycolide) Nanoparticles Suppresses the Development of Multidrug Resistance in K562 Cells

Ranjita Misra and Sanjeeb K. Sahoo*

Institute of Life Sciences, Nalco Square, Chandrasekharpur, Bhubaneswar, Orissa, India

ABSTRACT: Doxorubicin (DOX) is a broad-spectrum anthracycline antibiotic used to treat a variety of cancers including leukemia. Chronic myeloid leukemia (CML) blasts like K562 cells are resistant to apoptosis induced by DOX due to several reasons, the primary being the sequestration of drug into cytoplasmic vesicles and induction of multidrug resistance (MDR) gene expression with DOX treatment resulting in intracellular resistance to this drug. Moreover, expression of antiapoptotic protein BCL-2 and the hybrid gene bcr/abl in K562 cells contributes resistance to DOX. Studies have shown that curcumin (CUR) has a pleiotropic therapeutic effect in cancer treatment, as it is an inhibitor of nuclear factor kappa B (NFκB) as well as a potent downregulator of MDR transporters. In this study, we investigated the potential benefit of using DOX and CUR in a single nanoparticle (NP) formulation to inhibit the development of drug resistance for the enhancement of antiproliferative activity of DOX in K562 cells. Results illustrate that the dual (DOX+CUR) drug loaded NPs were effectively delivered into K562 cells. CUR not only facilitates the retention of DOX in nucleus for a longer period of time but also inhibits the gradual expression of MDR1 and BCL-2 at the mRNA level in K562 cells. Moreover, Western blot results confirm that in combination both of the drugs were capable of inducing apoptosis even if in a lower concentration compared to either single drug in both solution or in formulation. Combinational therapy by using DOX and CUR, especially when administered in the NP formulation, has enhanced the cytotoxicity in K562 cells by promoting the apoptotic response. Overall, this combinational strategy has significant promise in the clinical management of intractable diseases, especially leukemia.

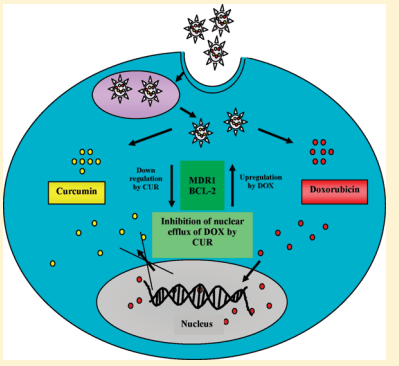

KEYWORDS: doxorubicin, curcumin, K562 cells, nuclear efflux, BCL-2, bcr/abl, dual drug loaded NPs

INTRODUCTION

Doxorubicin (DOX), a common anthracycline antibiotic, is often used for the treatment of various cancers, especially breast, ovarian, prostate, brain, lung and leukemia.[1−4] However, the efficacy of DOX is often compromised by multidrug resistance (MDR) mechanisms involving the P-glycoprotein (P-gp) proteins. DOX is in fact a substrate for drug transporters such as P-gp protein (MDR1) and multidrug resistance protein-1 (MRP1).[5] DOX is a weak base with a pK_a near neutrality; it is prone to accumulating in acidic cytoplasmic vesicles of cancer cells by active transport mechanisms, thereby creating sink conditions in the cytosol of some cancer cells.[6] Cytosolic sink conditions could facilitate DOX unbinding from intracellular targets present in cancer cells. In addition to active transport mechanisms, ion-trapping in low-pH compartments can mediate intracellular drug sequestration, leading to decreased sensitivity of DOX to cancer cells.[7,8]

Human chronic myelogenous leukemia (CML) is a malignancy of pluripotent hematopoietic cells that is caused by the dysregulated activity of the tyrosine kinase encoded by the chimeric bcr/abl oncogene.[9] The human CML cell line K562 is one of the most aggressive cell lines that exhibit an apoptosis-resistant phenotype upon the action of most antiproliferative agents including DOX.[2] K562 cells sequester DOX in cytoplasmic vesicles and intrinsically become more resistant to it.[7,8] Moreover, expression of low levels of MDR transporters in K562 cells leads to resistance to DOX-induced cytotoxicity. These MDR transporters can facilitate the intracellular drug sequestration and may contribute to the acquisition of MDR.[7,8] Furthermore, Hui et al. have reported that DOX treatment induces MDR1 mRNA expression in K562 cells.[10] It has been also reported that expression of antiapoptotic gene BCL-2 in many cancer cells leads to drug resistance including K562 cells.[11] Thus, the cause of DOX resistance is understood to be multifactorial with intracellular drug sequestration, expression of bcr/abl gene and gradual expression of MDR1 and BCL-2 at the mRNA level being the major factors that can contribute to intrinsic drug resistance of K562 cells.

Curcumin (CUR), a natural polyphenol, found in the rhizomes of *Curcuma longa* (turmeric), exhibits anti-inflammatory, antineoplastic, antioxidant and chemopreventive activities and

Received: December 24, 2010
Accepted: April 11, 2011
Revised: April 8, 2011
Published: April 11, 2011

ACS Publications © 2011 American Chemical Society

has been shown to be pharmacologically safe even at high doses.[12,13] It has been well-known that CUR inhibits the proliferation of several tumor cells due to its blocking activity of the transcriptional factor NFκB.[14] It has several different molecular targets within the MAPK and PI3K/PKB signaling pathways that could contribute to inhibition of proliferation and induction of apoptosis *in vitro* including K562 cells. Therefore, it is proposed that CUR may suppress tumor promotion by blocking signal transduction pathways in the target cells. Additionally, CUR is a potent inhibitor of three major ATP-binding cassette (ABC) drug transporters, MDR1, MRP1 and ABCG2, that are important in MDR.[15−17] Previous works have reported that CUR also inhibited the activity of p210bcr/abl tyrosine kinase in K562 cells.[18] Despite these promising pharmacological properties, CUR, owing to its extremely low aqueous solubility, is still in the clinical stages. Recently our group has developed different water based nanoformulations of CUR and has evaluated its enhanced cytotoxicity toward different cancer cell lines compared to its native form.[19,20]

Combinational drug treatments have played a prominent role in the treatment of CML.[21] It has been shown that most of the antileukemic drugs exert either synergistic or additive or even antagonistic effects in bcr/abl expressing cell lines like K562.[21,22] Tumor-targeted nanomedicines have also been used for "coformulating" chemotherapeutics, i.e. for delivering two different pharmacologically active agents to tumors simultaneously.[23] Recently, Sengupta and colleagues demonstrated that a nanocell encapsulating an antiangiogenic agent combrestatin and the cytotoxic drug doxorubicin was significantly more effective in inhibiting tumor growth than all relevant control regimens.[24] Ganta et al. have examined the combination delivery of paclitaxel and curcumin encapsulated in flaxseed oil containing nanoemulsions, for enhancement of efficacy in drug sensitive SKOV3 and resistant SKOV3/TR human ovarian adenocarcinoma cells.[16] It has been reported that CUR effectively synergized with different anticancer drugs in some leukemic cancer cell lines.[9,25,26] It is also noteworthy that CUR efficiently inhibits the expression of MDR1, BCL2 and bcr/abl gene in K562 cells.[16,18,27] Detailed analysis of the problem led us to formulate the hypothesis that coadministration of DOX and CUR in a single formulation may inhibit the efflux of DOX from the nucleus and also decrease the expression of MDR1, BCL-2 and bcr/abl gene leading to enhanced therapeutic efficacy of DOX in K562 cells. To verify our hypothesis, we have studied the codelivery of DOX and CUR in poly(D,L-lactide-*co*-glycolide) (PLGA) NPs, for enhancement of efficacy of DOX in K562 cells. Encapsulation of both DOX and CUR in PLGA NPs helps in improving the solubility and stability of both the hydrophobic drugs, thereby circumventing the pitfalls of poor solubility and consequently protecting them from hydrolytic degradation and biotransformation. This paper presents the results of a series of experiments in which we have examined the efficacy of the constructed dual drug loaded NPs as an anticancer agent. We have evaluated the intracellular delivery of DOX and downregulation of MDR1 and BCL-2 gene expression with the help of CUR in K562 cells. In addition to this, we have also studied the enhancement of cell-kill efficacy, and the apoptotic response following treatment with dual drug loaded NPs in K562 cells. Thus, here we provide the proof-of-principle for multidrug targeting in a single drug carrier system for leukemia therapy. Our long-term goal involves site specific drug delivery by active targeting of this novel dual drug loaded formulation anticipating that this system can become a promising target for treatment of leukemia.[28]

MATERIALS AND METHODS

Poly(D,L-lactide-*co*-glycolide) (PLGA, copolymer ratio 50:50, I.V. = 0.55−0.75) was purchased from Birmingham Polymers, Inc. (Birmingham, AL). Polyvinyl alcohol (PVA, average MW 30,000−70,000), doxorubicin hydrochloride (DOX-HCL), 3-[4,5-dimethylthiazol-2-yl]-2,5-diphenyltetrazolium bromide (MTT), RNase and propidium iodide were obtained from Sigma-Aldrich (St. Louis, MO, USA). CUR-500, containing curcumin (>95%), was purchased from UNICO Pharmaceuticals, Ludhiana, India. Sodium chloride, disodium hydrogen phosphate, potassium bromide and potassium chloride were obtained from Sigma-Aldrich Chemicals, Germany. Potassium hydrogen phosphate was purchased from Qualigens Fine Chemicals (Mumbai, India). Chloroform, dichloromethane, methanol, acetonitrile and acetic acid were purchased from E-merk (India). All primary antibodies and horseradish peroxidase-conjugated secondary antibodies were purchased from Santa Cruz Biotechnology (Santa Cruz, CA, USA). All reagents used were of analytical grade from E-merk (India).

Preparation of Drug Loaded NPs. At first doxorubicin hydrochloride was converted to its free base by using our previous protocol.[29] NPs containing DOX and CUR were formulated by using single emulsion solvent evaporation technique.[30] In brief, a solution containing 100 mg of PLGA polymer, 5 mg of DOX and 5 mg of CUR in 3 mL of 12.5% (v/v) methanol in chloroform solution (12.5:87.5) was emulsified in 12 mL of 2% (w/v) aqueous solution of PVA to form an oil-in-water emulsion. The emulsification was carried out using a microtip probe sonicator set at 55 W of energy output (VC 505, Vibracell Sonics, Newtown, CT, USA) for 2 min over an ice bath. The emulsion was stirred overnight at room temperature on a magnetic stir plate to allow evaporation of organic solvent and formation of NPs. NPs were recovered by ultracentrifugation at 40,000 rpm for 20 min at 4 °C (Sorvall Ultraspeed Centrifuge, Kendro, USA) and washed twice with double distilled water to remove unbound PVA and unencapsulated free DOX and CUR, followed by lyophilization for 2 days (−80 °C and <10 μm mercury pressure, LYPHLOCK 12, Labconco, Kansas City, MO) to get the powdered form of NPs. Single drug formulation (either DOX or CUR) were prepared by using a similar procedure.

Particle Size Analysis and Zeta Potential Measurement. Dynamic laser scattering (DLS) was used to measure the hydrodynamic diameter (d nm), and laser Doppler anemometry (LDA) was used to determine zeta potential (mV). The DLS and LDA analyses were performed using a Zetasizer Nano ZS (Malvern Instruments, Malvern, U.K.). To determine the particle size and zeta potential, a dilute suspension of NPs (100 μg/mL) was prepared in double distilled water, sonicated on an ice bath for 30 s and subjected to particle size and zeta potential measurement using a Zetasizer (Nano ZS, ZEN 3600, Malvern Instrument, U.K.). All measurements were performed in triplicate.

Scanning Electron Microscope (SEM) Studies. The surface morphology of NPs was characterized by SEM (JEOL JSMT220A scanning electron microscope, Peabody, MA, USA) operating at an accelerating voltage of 10−30 kV. The NPs were sputtered with gold to make them conductive and placed on a copper stub prior to the acquisition of SEM images.

Atomic Force Microscope (AFM). The shape of NPs was further characterized by AFM (JPK Nanowizard II, JPK

Instruments, Bouchéstrasse, Berlin, Germany) consisting of pyramidal cantilevers with silicon probes having force constants of 0.2 N/m. Samples for AFM imaging were prepared by placing a drop of NP suspension (1 mg/mL) on a freshly cleaved mica sheet. After 5 min of incubation, the surface was gently rinsed with deionized water to remove unbound NPs. The sample was air-dried at room temperature and mounted on the microscope scanner. The shape was observed and imaged in contact mode set at a frequency of 13 kHz and scanned at a speed of 1 Hz. The images were analyzed using JPK data processing software.

Transmission Electron Microscope (TEM) Studies. The internal structure of NPs was determined by TEM (Philips/FEI Inc., Briarcliff Manor, NY). For this, NPs (100 μg/mL) were suspended in water and sonicated for 30 s. One drop of this suspension was placed over a carbon coated copper TEM grid (150 mesh, Ted Pella Inc., Redding, CA), negatively stained with 1% uranyl acetate for 10 min, and allowed to dry, and the images were visualized at an accelerating voltage of 120 kV under a microscope.

Assessing the Entrapment Efficiency of DOX and CUR. The amount of DOX entrapped in either single or dual drug loaded NPs was estimated by fluorescence spectrophotometer (Synergy HT, BioTek Instruments Inc., Winooski, VT). The amount of CUR encapsulated in either single or dual drug loaded NPs was estimated by the reverse phase isocratic mode of high performance liquid chromatography (RP-HPLC) using Waters 600, Waters Co. (Milford, MA, USA). Briefly, ~1 mg of lyophilized drug loaded NPs was dissolved in 1 mL of 12.5% (v/v) methanol in chloroform solution. The solution was sonicated for 1 min in an ice bath and centrifuged for 10 min at 13,800 rpm at 4 °C (SIGMA 1-15K, Germany). The supernatant was used to estimate the DOX concentration in NPs by fluorescence spectrophotometer at λex = 485 nm and λem = 591 nm.[29] A standard plot of DOX was prepared previously in the same conditions to calculate the amount of DOX entrapped in the NPs. For CUR estimation, the supernatant obtained was analyzed by RP-HPLC. For this, 20 μL of supernatant was injected manually in the injection port of HPLC and was analyzed using a mobile phase of acetonitrile, acetate buffer (20 mM, pH 3.0) and methanol in the ratio of 60:10:30, v/v. Triethylamine (3 mM) was added in the mobile phase to decrease the tailing of the peak.[31] The mobile phase was delivered at a flow rate of 1 mL/min with a quaternary pump (M600E WATERS) at 25 °C with a C 18 column (Nova- Pak, 150 × 4.6 mm, internal diameter). Curcumin levels were quantified by UV detection at 420 nm with dual wavelength absorbance detector (M 2489). The amount of CUR in NPs was determined from the peak area correlated with the standard curve. The standard curve of CUR was prepared under identical conditions. All analysis was performed in triplicate. The encapsulation efficiency of either DOX or CUR was calculated by dividing the amount of drug entrapped by the total amount of drug added, multiplied by 100.[20]

***In Vitro* Release Kinetics Study.** *In vitro* release of either DOX or CUR from NPs (both single and dual drug loaded formulation) was carried out by dissolving 10 mg of NPs in 3 mL of PBS (0.01 M, pH 7.4) containing 0.1% v/v of Tween 80 (to maintain a sink condition).[32] The NP suspension was equally divided in three tubes containing 1 mL each (as the experiment was performed in triplicate) and kept in a shaker at 37 °C at 150 rpm (Wadegati Labequip, India). At particular time intervals, these tubes were taken out from shaker and centrifuged at 13,800 rpm, 4 °C for 10 min (SIGMA 3K30, Munich, Germany). To the pellet obtained after centrifugation, 1 mL of fresh PBS/Tween 80 solution was added to the shaker for the next readings. The collected supernatant was lyophilized and dissolved in 1 mL of 12.5% (v/v) methanol in chloroform solution. The solution was centrifuged at 13,800 rpm for 10 min at 25 °C to collect the drug in the supernatant. The amount of DOX and CUR in the sample was determined by fluorescence spectrophotometer and HPLC respectively as described previously to determine the amount of drug released with respect to different time intervals.

Fourier Transform Infrared (FTIR) Spectral Studies. The chemical integrity of the drug and the polymeric matrix was investigated using FTIR spectra (Perkin-Elmer, Model Spectrum1, California, USA). Samples were crushed with KBr to get the pellets by applying a pressure of 300 kg/cm^2. FTIR spectra of both DOX and CUR single or in combination both in native and in NP formulation were scanned in the range between 4000 and 500 cm^{-1}.

Cell Culture. Human leukemia cell line (K562) was kindly provided by Dr. Soumen Chakrobarty, Scientist, at Institute of Life Sciences, Bhubaneswar, India, and cultured using RPMI 1640 with 10% FBS, 1% L-glutamine and 1% penicillin—streptomycin at 37 °C in a humidified, 5% CO_2 atmosphere maintained in an incubator (Hera Cell, Thermo Scientific, Waltham, MA). All chemicals for cell culture were purchased from PAN Biotech, (GmbH, Germany).

Cellular Uptake Study by Flow Cytometry. Cellular uptake efficiency of different formulations of DOX in K562 was measured by flow cytometry.[28] Briefly, 1 × 10^5 cells per well were seeded in 12-well plates (Corning Inc., Corning, NY) 24 h before the experiment. Cells were treated with 1 mL of freshly prepared equivalent concentration of DOX (1 μg/mL) either in (DOX + CUR) in solution or in nanoparticular formulation {(DOX + CUR)-NPs} and incubated for 2 h at 37 °C in CO_2 incubator (Hera Cell, Thermo Scientific, Waltham, MA). Cells treated with only medium were used as respective control. At the end of the incubation period, the cells were then collected by centrifugation at 1000 rpm (SIGMA 3K30, Munich, Germany) and washed three times with cold DPBS (PAN Biotech, GmbH, Germany) to eliminate excess of free drug or unbound NPs and the amount of NPs uptake was analyzed by FACS (FACScan flow cytometer, Becton Dickinson). In all FACS analysis, cell debris and free particles were excluded by setting a gate on the plot of side-scattered light (SSC) vs forward-scattered light (FSC). A total of 10,000 gated cells were analyzed for the study. The increase of fluorescence in the cells treated with NPs relative to that in the untreated control cells was expressed as mean fluorescence intensity relative to control.

Cellular Uptake of DOX in K562 Cells by Fluorescence Spectrophotometer. Cellular uptake of different formulations of DOX in K562 cells was studied by fluorescence spectrophotometer.[29] For this, 1 × 10^6 cells were seeded in T-25 flasks (Corning, NY, USA) 24 h before experiment. The cells were treated with 5 mL of solution containing equivalent concentration of DOX (10 μg/mL) either in the form of DOX or (DOX + CUR) in solution or in formulation {DOX-NPs and (DOX + CUR)-NPs} and incubated for 2 h at 37 °C in CO_2 incubator (Hera Cell, Thermo Scientific, Waltham, MA). The concentration of CUR in dual drug loaded NPs is 18.9 μg/mL. Cells were washed three times with DPBS (PAN Biotech, GmbH, Germany) to remove the excess of unbound drugs and then incubated with 0.1 mL of 1 X cell lysis reagent (Sigma-Aldrich, St. Louis, MO, USA) for 20 min at 37 °C. Five microliters of cell

lysate was used for cell protein determination using micro BCA protein assay (Pierce, Rockford, IL, USA), and the remaining portion was lyophilized. DOX from the lyophilized NPs was extracted by dissolving each sample in 1 mL of 12.5% (v/v) methanol in chloroform solution.[29] The samples were centrifuged at 13,800 rpm for 10 min in a microcentrifuge tube to remove cell debris. The supernatant was analyzed for DOX, using a fluorescence spectrophotometer (Synergy HT, BioTek Instruments Inc., Winooski, VT). A standard plot with different concentration of NPs was constructed simultaneously under similar conditions to determine the amount of NPs in cell lysate. The data was normalized micrograms of DOX per milligram of cell protein.[29]

Nuclear Efflux of DOX in K562 Cells by Fluorescence Spectrophotometer. We have evaluated the efflux of DOX in different formulations from the nucleus of K562 cells by using our previous protocol.[29] Briefly, 1×10^6 cells were seeded in T-25 flasks (Corning, NY, USA) 24 h before the experiment. Cells were pulsed with an equivalent concentration of DOX (10 μg/mL), either DOX in solution or (DOX+CUR) in solution or in formulation {DOX-NPs and (DOX+CUR)-NPs} in culture medium for 2 h at 37 °C. The concentration of CUR in dual drug loaded NPs is 18.9 μg/mL. Following the pulse, cells were washed twice with fresh culture medium and incubated in drug-free medium up to 2−8 h. To determine the amount of DOX efflux out from the nucleus at predetermined time interval, the cells were washed three times with DPBS (PAN Biotech, GmbH, Germany). Cytoplasm and nuclei were collected separately, as described in our previous paper.[26] Five microliters of cell lysate was taken for cell protein estimation using micro BCA protein assay (Pierce, Rockford, IL, USA). The concentration of DOX in cytoplasm or nucleus was determined by the fluorescence measurement. Cellular DOX levels were expressed as micrograms of DOX per milligram of protein.

MDR1 and BCL-2 Expression Study by RT-PCR. To study the expression of MDR1 and BCL-2 at the mRNA level in K562 cells, cells were treated with an equivalent concentration of DOX (10 μg/mL), either DOX in solution or (DOX+CUR) in solution or in formulation {DOX-NPs and (DOX+CUR)-NPs} for 96 h.[33] Briefly, 2.5×10^6 cells/10 mL were seeded in T-25 flasks (Corning, NY, USA) 24 h before the experiment. The concentration of CUR in dual drug loaded NPs is 18.9 μg/mL. Cells treated with medium served as control. Total RNA was extracted from the cultured cells using a QIAamp RNA blood mini kit (Qiagen, Hilden, Germany) according to the manufaturer's instructions. The reverse transcription reactions were performed using SuperScript II reverse transcriptase (Invitrogen Life Technologies, California, USA), and the newly synthesized cDNA was amplified within target and control sequences. The cDNA products of the reverse transcription reaction were amplified with Takara Ex Taq (Takara Sigha, Japan) using forward and reverse primers of MDR1 and BCL-2 gene to produce product of the human MDR1 and BCL-2 sequence. The relative gene copy number was calculated by the concentration−CT standard curve method and normalized using the average expression of β-actin.

Cytotoxicity Study. The cytotoxicity studies were performed with both free drug and the NP formulations containing different ranges of concentrations of free drug {DOX and (DOX+CUR)} in solution or in formulation {DOX-NPs and (DOX+CUR)-NPs} by MTT based colorimetric assay.[34] Approximately 3,000 cells per well were seeded into 96-well plates (Corning, NY, USA) 24 h before the experiment. Cells were treated with increasing concentrations (ranging from 0.001 μg/mL to 20 μg/mL) of the drug for 48 h. Controls included the blank NP formulations and growth media. At the end, the medium was removed and 100 μL of fresh medium was added along with 10 μL of MTT reagent (5 mg/mL, Sigma) and incubated for 3 h in a CO_2 incubator (Hera Cell, Thermo Scientific, Waltham, MA). The medium was then aspirated and the formazan crystals were dissolved in 100 μL of dimethyl sulfoxide. The relative percentage of metabolically active cells relative to untreated controls was then determined on the basis of the mitochondrial conversion of 3-(4, 5-dimethylthiazol-2-yl)-2,5-diphenyltetrazolium bromide to formazan. The results were assessed in a 96-well format ELISA plate reader (Synergy HT, BioTek Instruments Inc., Winooski, VT, USA) by measuring the absorbance at a wavelength of 540 nm. The percentage of metabolically active cells was compared with the percentage of control cells growing in the absence of drug in the same culture plate. The IC_{50} was determined by nonlinear regression analysis using the equation for a sigmoid plot.

Table 1. Physicochemical Characteristics of NP Formulation

formulation	size[a] (nm)	polydispersity index	zeta potential[b] (mV)	encapsulation efficiency[c] (%)
DOX-NPs	226 ± 3.9	0.11 ± 0.004	−14.3 ± 1.4	49
CUR-NPs	239 ± 2.1	0.15 ± 0.005	−14.1 ± 1.2	83
DOX+CUR loaded NPs	248 ± 1.6	0.18 ± 0.009	−12.3 ± 5.1	46[d] 86[e]

[a] Size in nm as measured by dynamic laser spectroscopy. [b] Zeta potential in mV as measured by zetasizer. [c] Encapsulation efficiency of DOX (expressed as %) was estimated by fluorescence spectrophotometer, and encapsulation efficiency of CUR (expressed as %) was estimated by HPLC. [d] For DOX. [e] For CUR.

Cell Cycle Analysis by Flow Cytometry. The distribution of DNA in the cell cycle was studied by flow cytometry.[28] 5×10^5 cells/5 mL were seeded in a T-25 flask (Corning, NY, USA) 24 h before the experiment. The cells were exposed to either DOX in solution and DOX-NPs (1 μg/mL) or CUR in solution and CUR-NPs (2 μg/mL) or a combination of both drugs either in solution (DOX+CUR) or in formulation {(DOX+CUR)-NPs} having drug concentration in the proportion {(1 + 2) μg/mL} in culture medium and incubated for 48 h in CO_2 incubator at 37 °C. Cells treated with only medium were used as controls. After completion of the incubation period, the cells were washed with DPBS (PAN Biotech, GmbH, Germany) twice. The cells were resuspended in 500 μL of hypotonic propidium iodide solution, which consists of 1 μL of propidium iodide (10 μg/μL), 1 μL of RNase A (10 μg/μL, MP Biomedicals, Inc., Germany), and 0.5% Tween-20 in 500 μL of DPBS (PAN Biotech, GmbH, Germany), and incubated for 1 h at room temperature in the dark before analysis. Cell cycle distribution of the cells was determined by analyzing 10,000 ungated cells using a FACScan flow cytometer and Cell Quest software (FACS Calibur; Becton-Dickinson, San Jose, CA). All experiments were performed in triplicate.

Mitochondrial Membrane Depolarization Study. The study of mitochondria and changes in the mitochondrial membrane potential has become a focus of apoptosis analysis.[28] Lipophilic cation 5,5′,6,6′-tetrachloro-1,1′,3,3′-tetraethylbenzimidazol-carbocyanine iodide (JC-1) dye and flow cytometry

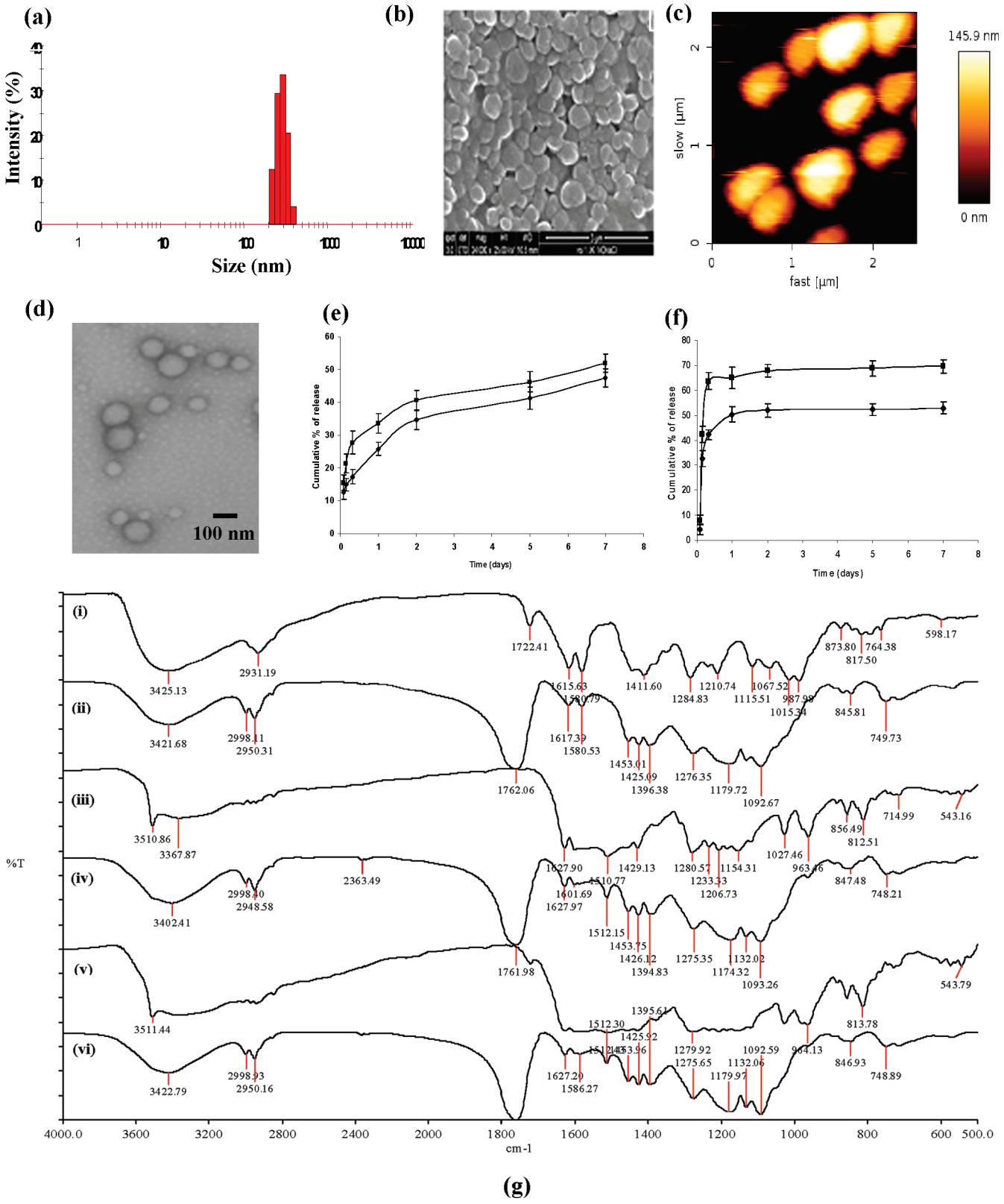

Figure 1. Physicochemical characterization of dual drug loaded NPs. (a) Size measured by dynamic laser spectroscopy. (b) Scanning electron micrograph of dual drug loaded NPs. (c) Size distribution of dual drug loaded NPs as measured by AFM. (d) Transmission electron microscopy of dual drug loaded NPs. (e) *In vitro* release of DOX either from DOX loaded NPs (■) or from DOX+CUR loaded NPs (◆) in PBS (0.01 M, pH = 7.4 containing 0.1% v/v of Tween 80). (f) *In vitro* release of CUR either from CUR loaded NPs (■) or from DOX+CUR loaded NPs (◆) in PBS (0.01 M, pH = 7.4 containing 0.1% v/v of Tween 80). (g) FTIR spectra of (i) native DOX, (ii) DOX-NPs, (iii) native CUR, (iv) CUR-NPs, (v) native (DOX+CUR) and (vi) (DOX+CUR)-NPs.

dx.doi.org/10.1021/mp100455h |*Mol. Pharmaceutics* 2011, 8, 852–866

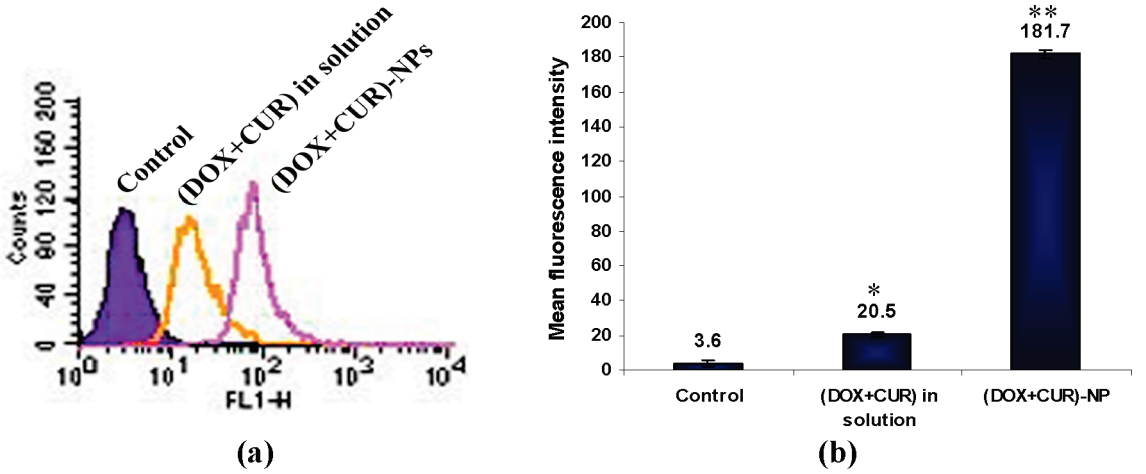

Figure 2. Cellular uptake by flow cytometry. (a) Cellular uptake study of equivalent concentration of DOX (1 μg/mL) either (DOX+CUR) in solution or in (DOX+CUR)-NPs measured by flow cytometry in K562 cells. (b) An enhanced uptake of NPs presented in terms of mean fluorescence intensity value. Data represented as mean ± SEM (n = 3). *p < 0.05, (DOX+CUR) in solution vs control. **p < 0.005, (DOX+CUR)-NPs vs control.

were used to analyze the mitochondrial membrane potential (MMP). As the color of the dye changes from orange to green, the membrane potential decreases. Briefly, 5 × 10^5 cells/5 mL were seeded in a T-25 flask (Corning, NY, USA) 24 h before the experiment. The cells were then exposed to different concentration of drugs either in solution or in formulation as mentioned in the earlier section on cell cycle analysis and incubated for 48 h in a CO_2 incubator at 37 °C. Cells treated with only medium were used as controls. After completion of incubation period, cells were washed twice with DPBS. The collected cells were treated with JC1 staining solution (3 μg/mL of JC-1 in DPBS warmed to 37 °C) and incubated at 37 °C for 20 min in a CO_2 incubator which exhibits potential-dependent accumulation in mitochondria. After the incubation period, cells were washed twice with DPBS. Ten thousand cells were examined for each sample on a FL-1 (530 nm) vs FL-2 (585 nm) dot plot using a FACScan flow cytometer and Cell Quest software (FACS Calibur; Becton-Dickinson, San Jose, CA). The experiment was performed in triplicate.

Western Blot Analysis. The molecular mechanism of apoptosis was demonstrated by Western blot analysis.[28] In brief, 2 × 10^6 cells were grown overnight at 37 °C in 25 cm^2 culture flasks (Corning, NY, USA) containing 5 mL of medium. To show the apoptotic effect of both the drugs (CUR and DOX), cells were exposed to different treatments in two sets. The effect of CUR was evaluated by treating the cells with CUR in solution (3 and 5 μg/mL), CUR-NPs (3 and 5 μg/mL), (DOX+CUR) in solution {(1 + 2) μg/mL} and (DOX+CUR)-NPs {(1 + 2) μg/mL} in 10 mL of medium. The effect of DOX was evaluated by treating the cells with DOX in solution (2 and 5 μg/mL), DOX-NPs (2 and 5 μg/mL), (DOX+CUR) in solution {(0.6 + 1.4) μg/mL} and (DOX+CUR)-NPs {(0.6 + 1.4) μg/mL} in 10 mL of medium, and the cells were incubated for 48 h at 37 °C. Cells treated with only culture medium served as control for the experiment. Next day, preparation of protein lysates and cell extracts was done by collecting the cells by centrifugation and washing in 1 X PBS followed by detergent lysis [50 mmol/L Tris-HCl (pH 8.0),150 mmol/L NaCl, 1% NP40, 0.5% Na-deoxycholate, 0.1% SDS, containing protease and phosphatase inhibitor (Sigma, St. Louis, MO) cocktails]. The soluble protein concentration was determined by the Pierce BCA protein assay

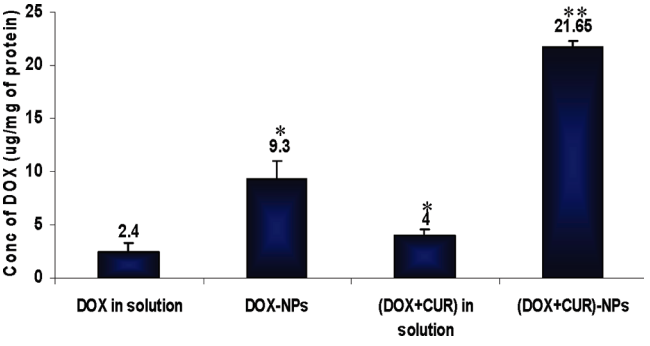

Figure 3. Total cellular uptake of DOX in K562 cells treated with DOX (10 μg/mL) either in DOX and (DOX+CUR) in solution or in NPs {DOX-NPs and (DOX+CUR)-NPs} for 2 h. Cellular uptake of DOX was quantified by measuring the fluorescence intensity. Data represented as mean ± SEM (n = 3). *p < 0.05, DOX-NPs vs DOX in solution and (DOX+CUR) in solution vs DOX in solution. **p < 0.005, (DOX+CUR)-NPs vs DOX in solution.

(Pierce, Rockford, IL). Aliquots of each sample containing 60 μg of proteins were resolved in SDS−polyacrylamide gel, and transferred to polyvinylidene difluoride membranes (Millipore Corp.). Membranes were then probed with primary antibody for 1 h (1:1000 dilutions). The membranes were reprobed with anti-β-actin antibody, as loading control after being stripped with stripping buffer. The membrane was washed three times with PBS containing 1% Tween-20 and probed with secondary antibody (1:5000 dilution) for 40 min. Proteins were visualized by using enhanced chemiluminescence detection reagents (Amersham Biosciences, Arlington Heights, IL) and exposed to Kodak life science imaging film (Kodak, USA). The experiment was repeated at least three times. All antibodies (primary and secondary) were obtained from Santa Cruz Biotechnology (Santa Cruz, CA).

bcr/abl Gene Expression Study by RT-PCR. In brief, 2.5 × 10^6 cells were grown overnight at 37 °C in 25 cm^2 culture flasks (Corning, NY, USA) containing 10 mL of medium. To show the apoptotic effect of both the drugs (CUR and DOX), cells were exposed to different treatments in two sets. The cells were exposed to different concentrations of drugs either in solution

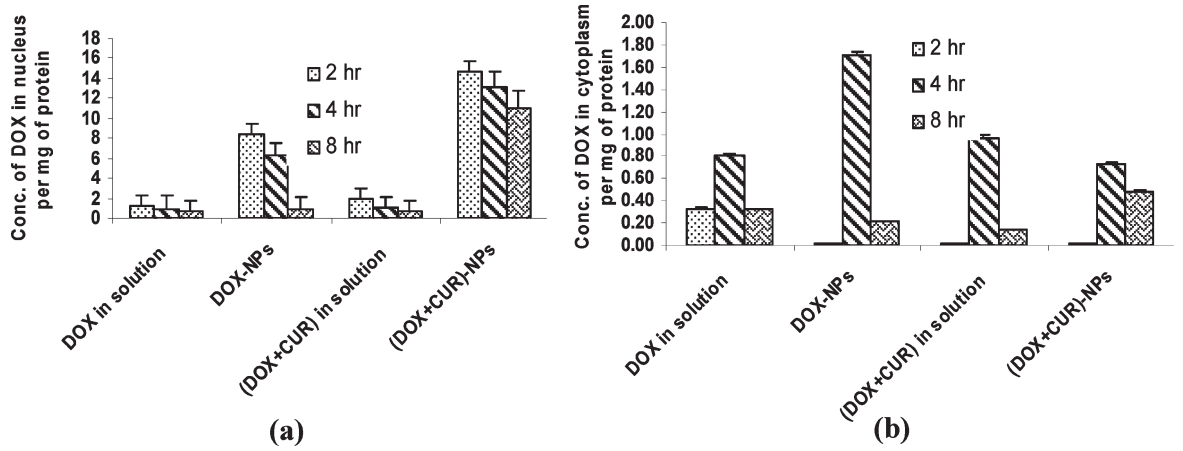

Figure 4. Efflux of DOX from the nucleus of K562 cells with different treatments of DOX and (DOX+CUR) in solution or in NP formulation for different time intervals (2, 4, and 8 h). (a) Concentration of DOX in the nucleus of cells after nuclear efflux for different incubation times. (b) Accumulation of DOX in cytoplasm for different time intervals.

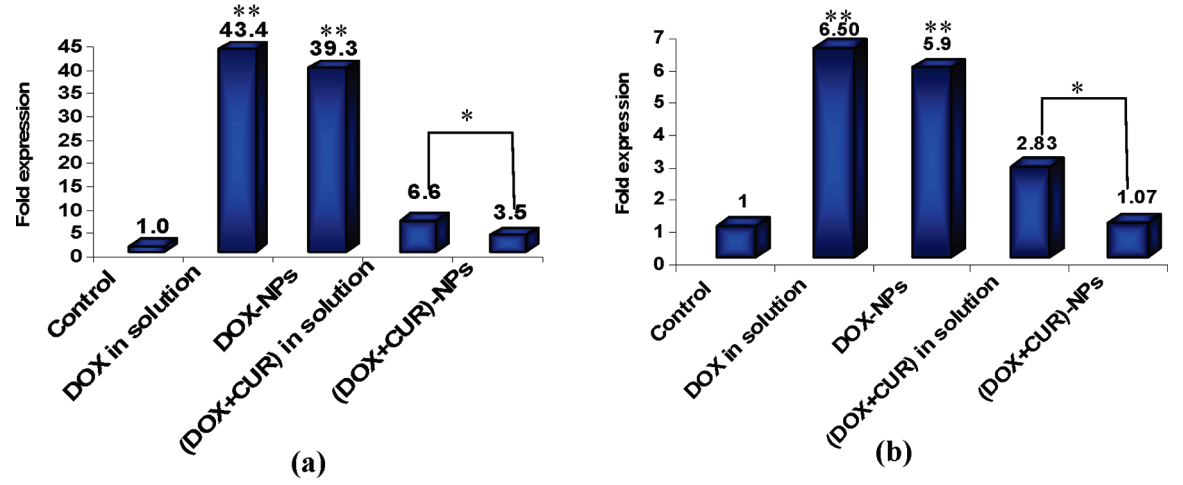

Figure 5. MDR1 and BCL-2 expression study by RT-PCR in K562 cells. (a) Role of CUR in inhibition of MDR1 gene expression with 96 h of DOX treatment in K562 cells, data represented as mean ± SEM (n = 3), *p < 0.05, (DOX+CUR)-NPs vs (DOX+CUR) in solution and **p < 0.005 (DOX+CUR)-NPs vs DOX in solution or DOX-NPs. (b) Role of CUR in inhibition of BCL-2 gene expression with 96 h of DOX treatment in K562 cells, data represented as mean ± SEM (n = 3), *p < 0.05, (DOX+CUR)-NPs vs (DOX+CUR) in solution and **p < 0.005 (DOX+CUR)-NPs vs DOX in solution or DOX-NPs.

or in formulation as mentioned in the earlier section on Western blot and incubated for 48 h at 37 °C. Cells not treated with any formulations served as control for the experiment. Total RNA was extracted from the cultured cells using a QIAamp RNA blood mini kit (Qiagen, Hilden, Germany) according to the manufacturer's instructions. The reverse transcription reactions were performed using SuperScript II reverse transcriptase (Invitrogen Life Technologies), and the newly synthesized cDNA was amplified within target and control sequences. The cDNA products of the RT reaction were amplified with Takara Ex Taq (Takara Sigha, Japan) using forward and reverse primers for bcr/abl gene to produce a 200 base pair product of the human bcr/abl sequence. The relative gene copy number was calculated by the concentration−CT standard curve method and normalized using the average expression of β-actin.[33]

Statistical Analysis. Statistical analyses were performed using a Student's t test. The differences were considered significant for p values of <0.05 and very significant for p values of <0.005.

RESULTS

Physicochemical Characterization of Drug Loaded NPs. Drug loaded NPs were prepared from PLGA polymer using a single emulsion method.[30] A successful NP system should have a high loading capacity to reduce the quantity of the carrier required for administration.[32] DOX and CUR were efficiently loaded in PLGA NPs, reaching a loading of 29 μg of DOX and 55 μg of CUR per mg of NP with encapsulation efficiency of 46% and 86% respectively (Table 1). Dynamic light scattering analysis revealed that the formulated NPs had an average diameter of 248 ± 1.6 nm (Figure 1a) with a negative zeta potential of −12.3 ± 5.1 mV. Moreover, surface morphology study of drug-loaded NPs by SEM showed that particles were spherical with a smooth exterior as evident from SEM results (Figure 1b). AFM studies confirmed the smooth and spherical surface of the formulated NPs along with the absence of aggregation or adhesion among NPs. The AFM technique was used to study the detailed

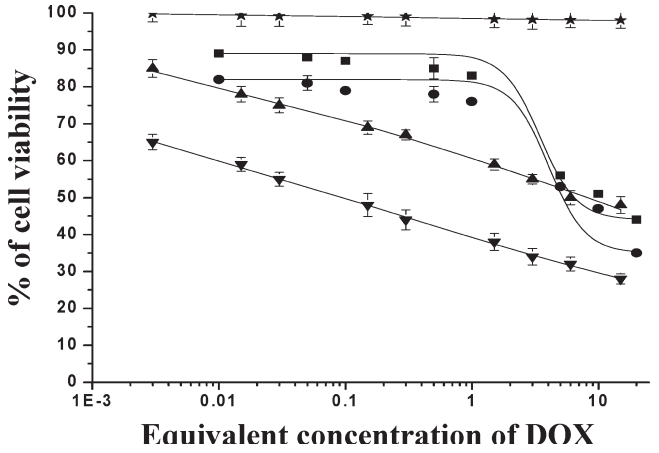

Figure 6. Dose dependent cytotoxicity of different concentration of void NPs (★), DOX in solution (■), DOX loaded NPs (◆), (DOX+CUR) in solution (▲) and (DOX+CUR)-NPs (▼) in K562 cells. The extent of growth inhibition was measured after 48 h using MTT assay. The percentage of survival was determined by standardizing the absorbance of controls to 100%.

Table 2. IC_{50} Doses of DOX in Solution or in Nanoformulation Either Single or in Combination with CUR in K562 Cells

sample	IC_{50}[a] (μg/mL)
DOX in solution	10.8 ± 0.95**
DOX-NPs	7.3 ± 0.88**
DOX equivalent in (DOX+CUR) in solution	6.7 ± 0.91**
DOX equivalent in (DOX+CUR)-NPs	0.1 ± 0.93

[a] Data as mean ± SEM, $n = 6$. **$p < 0.005$, DOX equivalent in DOX+CUR-NPs vs DOX in solution, DOX-NPs and (DOX+CUR) in solution.

morphology of NPs, as the prepared NPs are too small to be closely investigated by SEM due to its limited magnification. TEM images (Figure 1d) showed a discrete spherical outline and monodispersed size distribution of NPs. Both DOX and CUR showed sustained release kinetics from PLGA NPs as shown in Figure 1 e,f. Approximately 33% and 26% of DOX was released from DOX and DOX+CUR loaded NPs respectively after 24 h (Figure 1e), while 65% and 50% of CUR was released from CUR and DOX+CUR loaded NPs within 24 h respectively (Figure 1f). The initial burst release may be due to the diffusion of drugs present at or just beneath the surface of the NPs. The initial burst release was followed by a slower sustained release of drug present inside the core of NPs.[32]

FTIR analysis was used to characterize any chemical (formation of chemical bonds) changes that occurred in the polymer due to the addition of drug during the synthesis reaction. Figure 1g shows the FTIR spectra of native DOX, DOX-NPs, native CUR, CUR-NPs, native (DOX+CUR) and (DOX+CUR)-NPs. Spectral analysis of different samples showed characteristic bands due to different functional groups. The signature peaks at 1510 cm^{-1} and 1627 cm^{-1} found in native CUR and CUR-NPs are due to C═C double bonds and aromatic C═C double bonds respectively.[20] The signature peak at 1580 cm^{-1} observed in native DOX and DOX-NPs is due to aromatic N−H bending vibrations.[29] The peaks found in all the single formulations are present both in dual drug in native form and in nanoparticulate formulation indicating that both the drugs are present in native form without any chemical interaction with the polymer in dual drug loaded NPs.[35]

Cellular Uptake Study by Flow Cytometry. Using the intrinsic fluorescence property of DOX and CUR, a comparative analysis of intracellular uptake behavior of dual drug either in solution or in NP formulation was performed in the K562 cell line by flow cytometer (Figure 2a). The relative extent of cellular uptake was presented in terms of mean fluorescence intensity (MFI) exhibited by the cells. As evident from Figure 2b, the MFI values for dual drug in solution and in NP were 20.5 and 181.7 respectively. The result clearly indicates that cellular uptake of dual drug loaded NPs was nearly ~8 times higher than the dual drug in solution.

Cellular Uptake Study by Fluorescence Spectrophotometer. Intracellular uptake of different formulations of DOX (10 μg/mL) in K562 cells was determined by fluorescence spectrophotometer. Figure 3 depicts that DOX in NP formulation showed more cellular uptake than DOX in solution either single or in combination. Results showed that cells treated with dual drug loaded NPs showed 9 times higher cellular uptake of DOX than cells treated with DOX in solution, and 2.3 times more uptake of DOX was observed in comparison to single drug loaded NPs. It was also observed that dual drug in solution showed higher uptake than the single drug in solution. This may be due to CUR, which may help in higher cellular uptake of DOX leading to more cellular internalization of dual drug loaded NPs compared to other formulations.

Nuclear Efflux of DOX by Fluorescence Spectrophotometer. We determined the DOX concentrations inside nuclei and cytoplasm of K562 cells after treatment with different formulations of DOX. To investigate the differences in facilitated drug efflux from the nucleus, cells were pulsed with equivalent concentrations of DOX (10 μg/mL) either in solution {DOX and (DOX+CUR)} or in formulation {DOX-NPs and (DOX+CUR)-NPs} in culture medium for 2 h at 37 °C and then incubated in drug-free medium for 2, 4 and 8 h to allow drug efflux. The amount of drug in the nucleus was considerably higher during the initial period of time (2 h) compared to the later time period i.e. 8 h following the pulse in the case of all the treatments. It was also observed that maximum amount of DOX is accumulated in the nucleus with dual drug loaded NPs treated cells compared to other treatments (Figure 4a). After 4 and 8 h efflux conditions, the drug concentration in the nuclei of K562 cells had decreased drastically in cells treated with only either DOX in solution or DOX-NPs whereas the cells treated with dual drug loaded NPs showed maximum nuclear retention of DOX. We have also measured the concentration of DOX in the cytoplasm in the different given points and found that the amount of DOX in cytoplasm was less in the case of cells treated with dual drug loaded NPs compared to other treatments during 2 h, but after that the DOX concentration increases gradually with time, which means that in dual drug loaded NPs also DOX is effluxed out but in this case it occurs less compared to the other treatments (Figure 4b).

MDR1 and BCL-2 Expression Study by RT-PCR. To explore the potential role of CUR in inhibition of drug resistance in K562 cells after DOX treatment, we studied the expression of MDR1 and BCL-2 by RT-PCR in K562 cells over a 96 h time course. Hui et al. have reported that, with DOX treatment, the expression of MDR1 increases significantly in K562 cells with increasing time

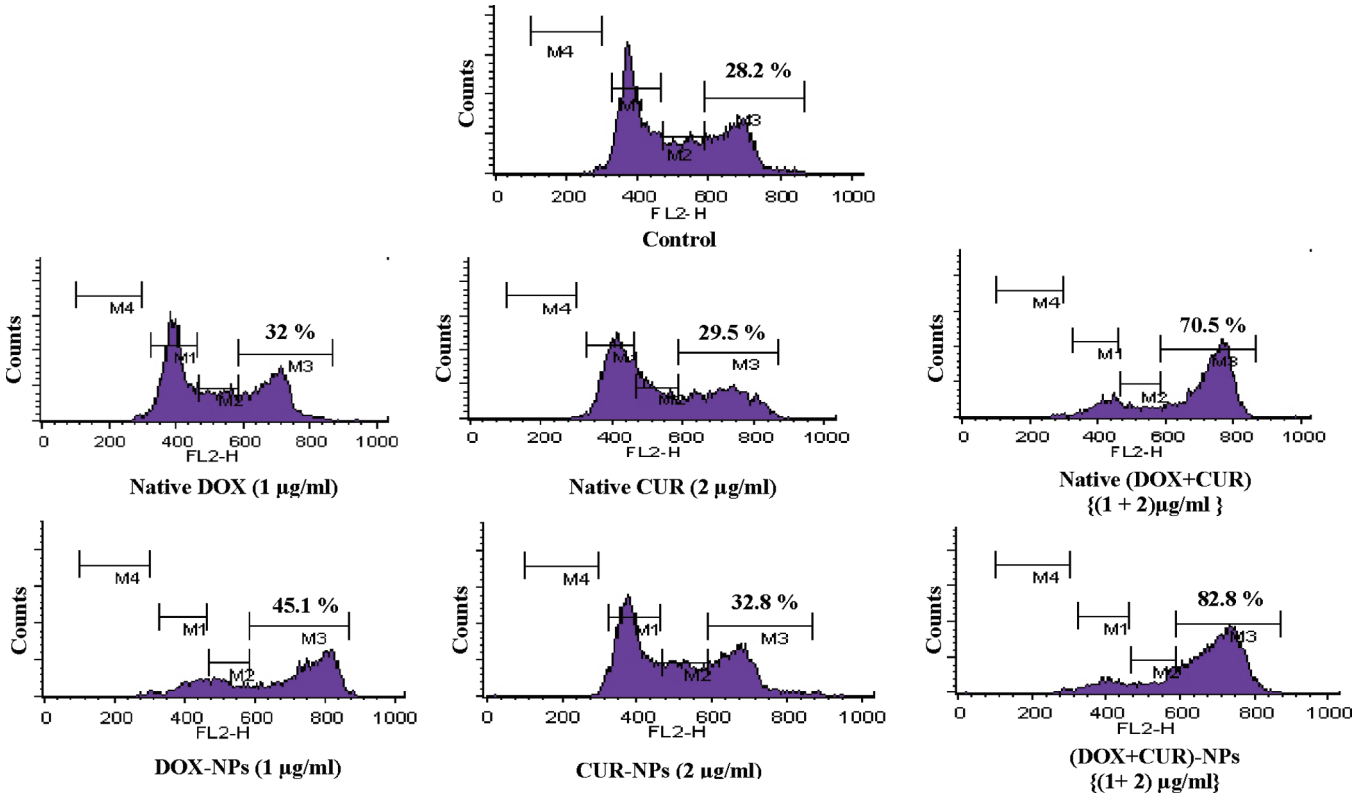

Figure 7. Cell cycle analysis by flow cytometry. Effect of different treatments {DOX in solution, CUR in solution, (DOX+CUR) in solution, DOX-NPs, CUR-NPs and (DOX+CUR)-NPs} on cell cycle distribution in K562 cells for 48 h. Content of DNA is represented on the *x*-axis; number of cells counted is represented on the *y*-axis ($n = 3$). The regions marked M1, M2, M3 and M4 represent G1, S, G2 and G0 phase, respectively, of the cell cycle. The results showed that (DOX+CUR)-NPs induce more G2/M blocking compared to other formulations.

of incubation. Figure 5 depicts that, upon DOX treatment, expression of both MDR1 and BCL-2 increases after 96 h of incubation. This leads to development of drug resistance in K562 cells. However, the NP formulations induce lower expression of both the genes compared to the single drug in solution. It was observed that dual drug loaded NPs inhibit further expression of both the resistant genes significantly compared to the drug in solution either single or in combination. It was also observed that, with dual drug loaded NP treatment, the expression of MDR1 and BCl-2 does not increases markedly, which means that CUR is helping in inhibition of expression of these two resistant genes leading to increasing efficacy of this formulation in K562 cells.

Cell Proliferation Assay. Therapeutic efficiency of drug loaded NPs is the outcome of their cellular uptake, intracellular distribution, and more importantly the amount of drug that is released from the internalized NPs inside the cell.[32] To investigate the therapeutic efficiency of these formulations, K562 cells were treated with different formulations of different concentrations for 48 h, and cell proliferation was measured by a standard MTT colorimetric assay.[36] It can be seen from Figure 6 and Table 2 that dual drug loaded NPs exhibited significantly higher cytotoxicity compared to drug in solution and single drug loaded NPs at all drug concentrations. The results depicted that when DOX is administered at equivalent concentrations, (DOX+CUR) loaded NPs exhibit lower IC_{50} value (0.1 μg/mL) among all the treatments and this showed approximately 100-fold higher effect in inhibiting cell growth than the drug in solution (IC_{50} = 10.8 μg/mL). This observation indicates that coadministration of DOX with CUR enhances the *in vitro* efficacy of the NP formulation synergistically.

Cell Cycle Analysis by Flow Cytometry. DOX and CUR inhibit cell growth and proliferation primarily through cell cycle arrest and apoptosis inducing mechanism.[13,21,37] Both DOX and CUR induce G2/M arrest in K562 cells.[38,39] To further confirm the therapeutic potential of combination therapy, cell cycle inhibition study was performed using flow cytometry. Figure 7 shows the relative cell cycle blocking activities upon treatment with single drug and combination of DOX and CUR in solution and in NP formulations. Both the NP formulations of DOX and CUR showed more cell cycle arrest at G2/M phase when compared to the respective drug in solution. We also compared the cell cycle arrest of dual drug loaded NPs and the dual drug in solution and found that the extent of cell cycle blocking is very high in dual drug NPs compared to all other formulations. These results corroborate with the cell viability data to confirm that NPs were effective in delivering the payload to the cells, and combination therapy with DOX and CUR delivered in NPs produced more potential therapeutic effects.

Mitochondrial Membrane Potential Study. The detection of the mitochondrial permeability transition event provides an early indication of the initiation of cellular apoptosis.[28] Loss of MMP can be detected by using JC-1 dye. Flow cytometry plots of K562 cells treated with different formulations (Figure 8) reveal that there was enhancement in membrane depolarization when DOX and CUR were administered in either single or combination NP formulations compared to the respective drugs in solution. In addition, when DOX and CUR were coadministered

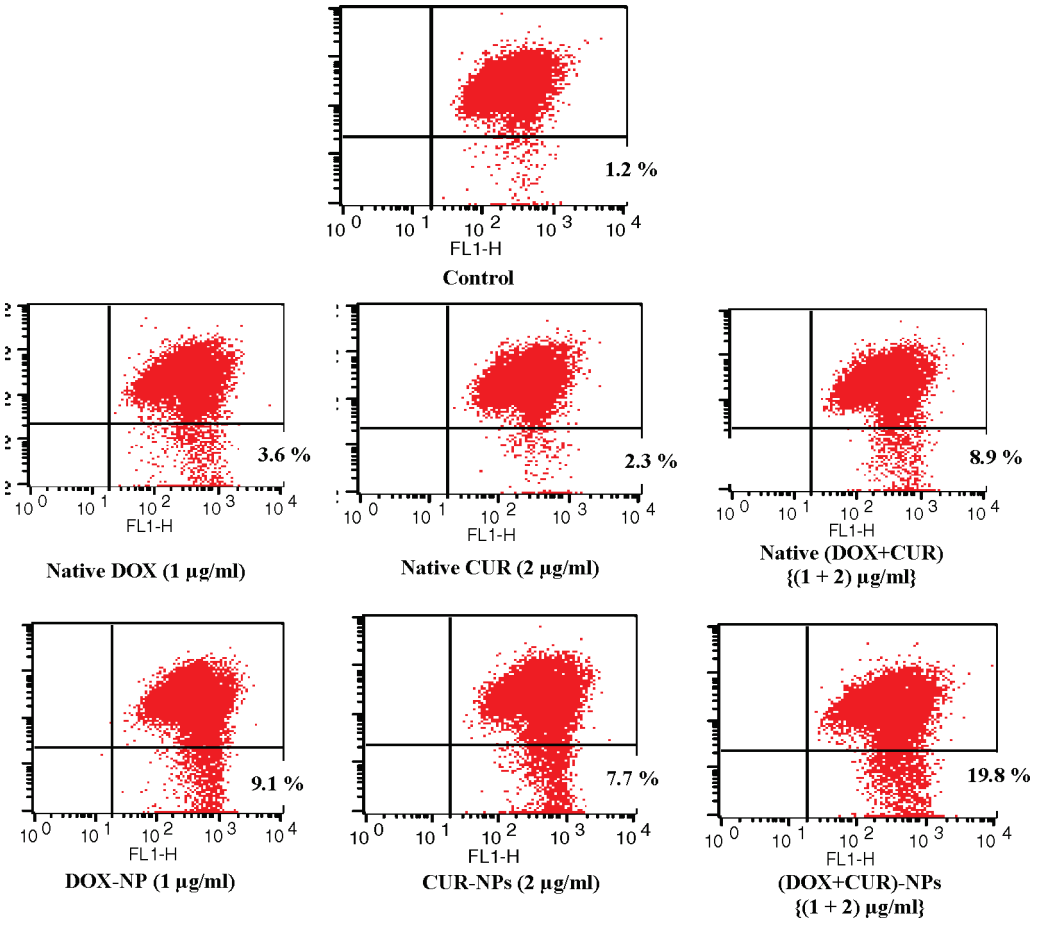

Figure 8. Detection of early induction of apoptosis was done using JC-1 dye by flow cytometry. Effect of different formulations in mitochondrial membrane depolarization in K562 cells. Data represented as mean ± SEM (n = 3). Cells treated with (DOX+CUR)-NPs formulation showed more mitochondrial membrane depolarization than cells treated with other formulations.

in NPs, there was an increase in membrane depolarization compared to all other formulations. Combination DOX and CUR therapy resulted in the highest degree of membrane depolarization due to combined action of both the drugs simultaneously in K562 cells.

Investigation of Apoptotic Proteins by Western Blotting. In this study, we have chosen two different concentrations (one lower and one higher) of different formulations to study the molecular mechanism of apoptosis in K562 cells (Scheme 1). In this experiment we have tried to show that both the drugs are combinedly acting to trigger apoptosis and are much more effective even if in lower concentration. Our results depicted that the combined formulations are much more effective (even if in much lower concentration) than that of both lower and higher concentrations of single drug in solution and in NP formulation. Figure 9 a and and Figure 9b depict that different formulations of CUR (designated as CUR) both single and in combination with DOX either in solution or in NP formulation are able to downregulate the NFκB pathway and bcr/abl induced Ras signaling pathway.[13,14,18,20] However, different formulations of only DOX (designated as DOX) as single agents have no effect on the expression of the above proteins. But, dual drug loaded NPs of both lower and higher concentrations are able to downregulate the NFκB pathway and bcr/abl induced Ras signaling pathway more prominently compared to all other formulations. The results also described that single CUR formulations of both lower (3 μg/mL) and higher (5 μg/mL) concentrations, either in solution or in NP formulation, are less effective than the dual drug loaded NPs containing lower concentration of DOX (1 μg/mL) and CUR (2 μg/mL) compared to their respective single formulations.

It is well established that both DOX and CUR displayed their activity by inducing mitochondrial apoptotic pathway.[13,40,41] As demonstrated in Figure 9c, dual drug loaded NPs of both lower and higher concentrations induced more cytoplasmic release of cytochrome c compared to all other formulations. This revealed that the combined effect of both DOX and CUR induced higher expression of mitochondrial apoptotic proteins leading to enhanced cytotoxicity of these dual drug loaded NPs. Similarly, the dual drug loaded NPs induced the expression of further downstream apoptotic proteins leading to enhanced apoptosis. In K562 cells DOX and CUR induced the cleavage of procaspase 8, which leads to induction of caspase 7 and caspase 3 leading to initiation of extrinsic apoptotic pathway (Figure 9d). In the same way as CUR, DOX formulations of both lower (2 μg/mL) and higher (5 μg/mL) concentrations, either in solution or in formulation, are less effective than the dual drug loaded NPs containing lower concentration of DOX (0.6 μg/mL) and CUR (1.4 μg/mL) compared to their respective single formulations. As a control, integrity β-actin was studied, and the quantities of β-actin protein were not affected by any of the cell treatments.

dx.doi.org/10.1021/mp100455h |*Mol. Pharmaceutics* 2011, 8, 852–866

Scheme 1. Schematic Representation of Different Apoptotic Pathways Induced by Both Curcumin and Doxorubicin[a]

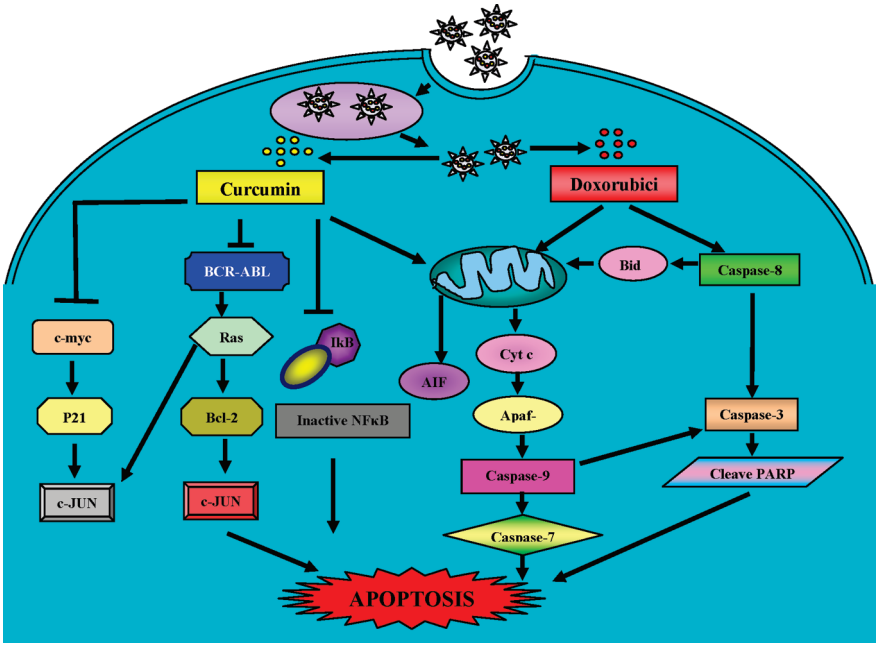

[a] After internalization of (DOX+CUR)-NPs into K562 cells, both the drugs are released inside the cells, inducing different apoptotic pathways, leading to more cytotoxicity. CUR inhibits the expression of bcr/abl gene, which ultimately leads to inhibition of the Ras signaling pathway. CUR also blocks the NFκB pathway, leading to apoptosis. Both DOX and CUR trigger the mitochondrial apoptotic pathway, leading to the release of cytochrome *c* from the mitochondria, which further helps in induction of caspase 9, caspase 3, and cleavage of PARP. Besides, these drugs also induce the release of apoptotic inducing factor (AIF), which directly induces apoptosis. DOX also induces the cleavage of procaspase 8, which leads to induction of caspase 7 and caspase 3. Activation of all these cumulative signaling pathways simultaneously results in apoptosis of K562 cells.

bcr/abl Gene Expression Study by RT-PCR. The development of CML mainly depends on the activity of bcr/abl gene.[42,43] We have evaluated the effect of the different formulations on the downregulation of bcr/abl gene by using RT-PCR. Figure 10 a depicts that different formulations of CUR both single and in combination with DOX either in solution or in formulation were able to downregulate the bcr/abl gene expression. Different formulations of only DOX were not able to downregulate bcr/abl gene expression, which means that DOX has comparatively less effect on the expression of bcr/abl gene (Figure 10b). The results showed that single CUR formulations of both lower (3 μg/mL) and higher (5 μg/mL) concentrations, either in solution or in formulation, were less effective than the dual drug loaded NPs containing lower concentration of DOX (0.6 or 1 μg/mL) and CUR (1.4 or 2 μg/mL) compared to their respective single formulations. However, marked reduction of bcr/abl gene expression was observed in the case of dual drug loaded NPs of both lower and higher concentrations compared to all other formulations.

DISCUSSION

K562 cells exhibit a significant level of intrinsic resistance to DOX. These cells have an active and well-characterized endocytic trafficking pathway with prominent multiple vesicular bodies (MVBs).[44,45] In these cells, the intralumenal vesicles of MVBs are released extracellularly as exosomes through fusion of MVBs with the plasma membrane.[8] Being a weak base with a pK_a near neutrality, DOX can accumulate in these acidic organelles leading to decreased cytotoxicity in K562 cells.[7,8] Another mechanism of resistance is due to expression of MDR1 and BCL-2 gene with gradual DOX treatment in K562 cells.[10,23] Moreover, a p210 bcr/abl mediated protection of K562 cells from the induction of apoptosis by cytotoxic drugs has been reported. All these reasons lead to lesser sensitivity of K562 cells toward DOX.[42,43,46,47]

Recently, CUR has been commonly studied as a magic drug due to its anticancer effect.[13,48] Several studies have demonstrated that CUR or CUR containing combination regimens are very effective in the treatment of cancer. Park et al. has demonstrated that CUR effectively reduced the growth of multiple myeloma (MM) cells and bone marrow stromal cells (BMSCs) by inhibiting IL-6/sIL-6R-induced STAT3 and Erk phosphorylation in the cocultured cells. They have reported that, in a combination treatment comprising CUR and bortezomib, IL-6/sIL-6R-induced STAT3 and Erk phosphorylation was effectively inhibited. Moreover, this combination treatment synergistically inhibited the growth of MM cells cocultured with BMSCs compared to controls, indicating that CUR potentiates the therapeutic efficacy of bortezomib in MM.[49] Zhang et al. have evaluated the synergistic inhibitory growth effect of PS-ASODN and CUR in K562 cells.[9] Ganta et al. have examined the coadministration of paclitaxel and CUR using nanoemulsion formulations that can aid in significant enhancement of cytotoxicity, especially in drug resistant SKOV3TR ovarian adenocarcinoma cells due to inhibition of NFκB activity and downregulation of important efflux transporters such as P-gp, and MRP-1 in tumor cells.[16]

In our study, CUR synergistically augmented the growth inhibitory effects of DOX in human leukemic cells *in vitro*. The rationale for selecting DOX and CUR for coencapsulation was

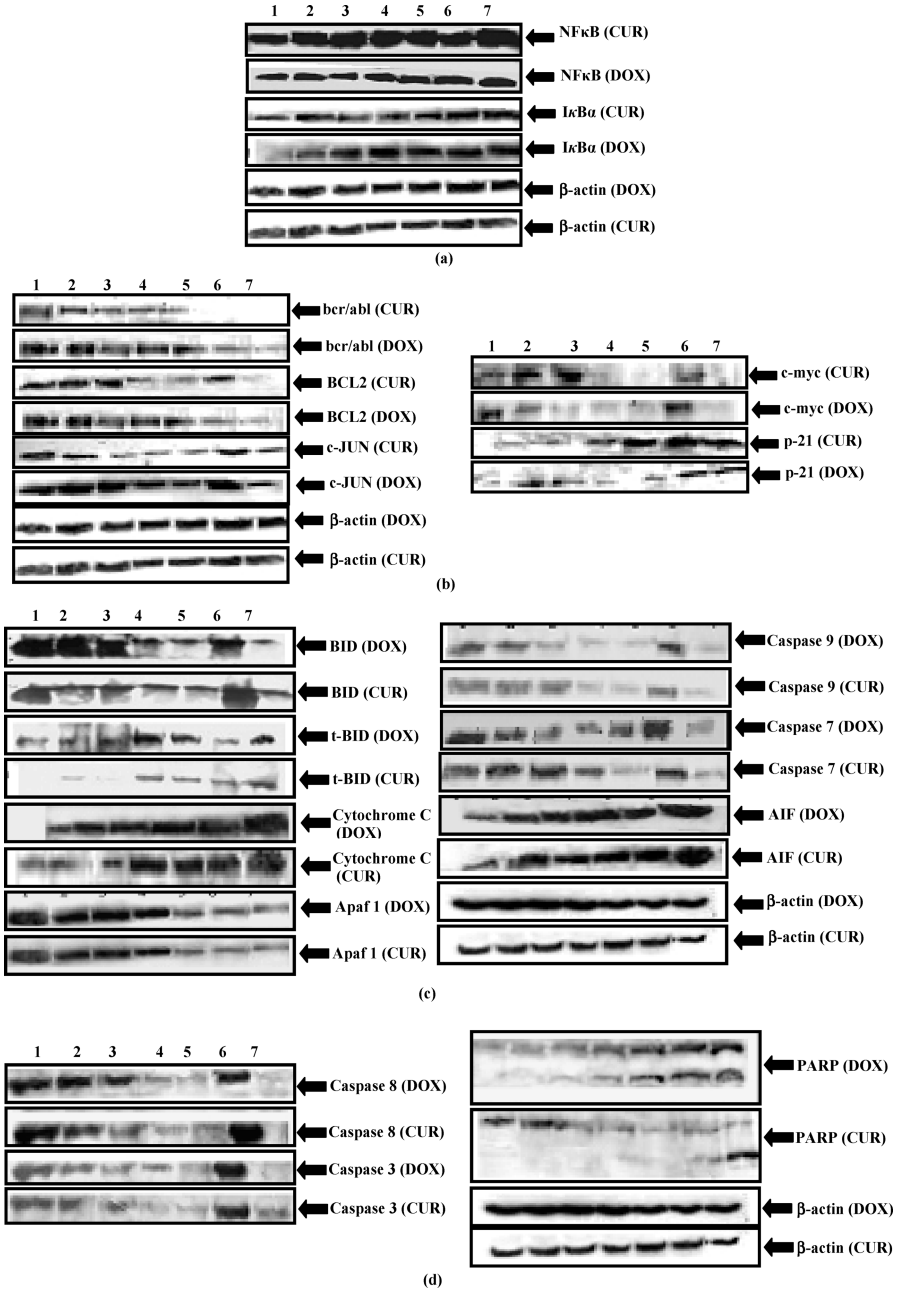

Figure 9. Western blot analysis of different proteins regulated by CUR and DOX involved in inducing different apoptotic pathways in K562 cells following treatment with different formulations. In CUR formulations (designated as CUR), lanes 1, 2, 3, 4, 5, 6, and 7 represent untreated control, CUR in solution (3 μg/mL), CUR in solution (5 μg/mL), CUR-NPs (3 μg/mL), CUR-NPs (5 μg/mL), (DOX+CUR) in solution $\{(1 + 2)\ \mu$g/mL$\}$ and (DOX+CUR)-NPs $\{(1 + 2)\ \mu$g/mL$\}$ treated K562 cells respectively. In DOX formulations (designated as DOX), lanes 1, 2, 3, 4, 5, 6, and 7 represent untreated control, DOX in solution (2 μg/mL), DOX in solution (5 μg/mL), DOX-NPs (2 μg/mL) and DOX-NPs (5 μg/mL), (DOX+CUR) in solution $\{(0.6 + 1.4)\ \mu$g/mL$\}$ and (DOX+CUR)-NPs $\{(0.6 + 1.4)\mu$g/mL$\}$ treated K562 cells respectively. β-Actin bands with the same intensity in all the lanes served as a loading control in this study. (a) Inhibition of NFκB pathway. High intense NFκB and IκBα bands were observed in all treated cells when compared to those of untreated cells. (DOX+CUR) loaded NPs further intensified the NFκB and IκBα bands compared to other treatments, suggesting that combo NPs were more efficient in enhancing the effect of CUR on the tumor cells. (b) Inhibition of bcr/abl induced downregulation of Ras signaling pathway. Results showed that combo formulation decreased the expression of p210bcr/abl resulting in downregulation of Bcl2 and c-JUN compared to each drug treated alone either in solution or in formulation. CUR also helps in inhibition of c-myc which ultimately leads to the higher expression of tumor suppressor protein p21 protein and finally downregulates the expression of c-JUN leading to apoptosis. (c) Induction of mitochondrial apoptotic pathway. Detection of cytochrome *c* and apoptosis-inducing factor (AIF) proteins after drug treatment indicates the activation of mitochondrial apoptotic pathway. (DOX+CUR)-NPs formulation was able to induce apoptosis in higher proportion compared to the other treatments. (d) Initiation of extrinsic apoptotic pathway after drug treatment by inducing cleavage of procaspase 8 leads to caspase 7, caspase 3 and PARP cleavage. As a control for the integrity, β-actin was detected in the supernatant, and the quantities of β-actin protein were not affected by any of the cell treatments.

dx.doi.org/10.1021/mp100455h |*Mol. Pharmaceutics* 2011, 8, 852–866

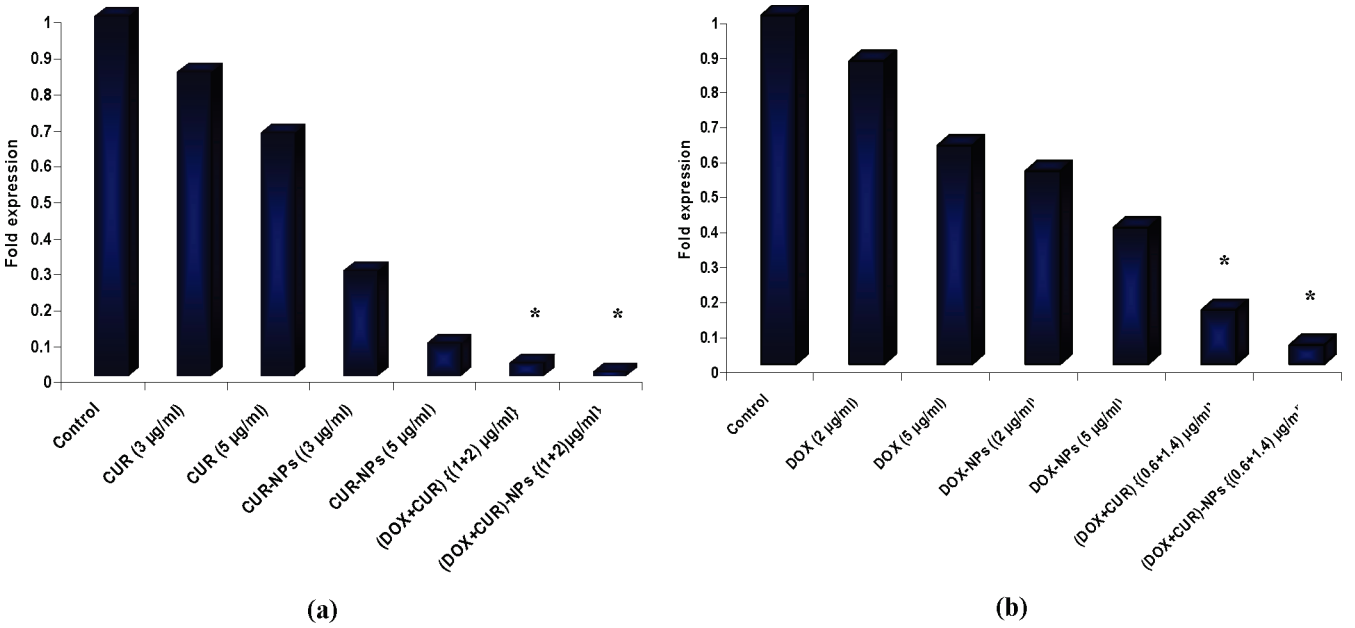

Figure 10. Downregulation of bcr/abl gene expression in K562 cells by RT-PCR after treatment with different concentration of DOX in solution, CUR in solution, (DOX+CUR) in solution, DOX-NPs, CUR-NPs and (DOX+CUR)-NPs for 48 h. (a) Decrease in fold expression of bcr/abl gene with CUR treatment data represented as mean ± SEM ($n = 3$), $^*p < 0.05$, control vs (DOX+CUR) in solution and (DOX+CUR)-NPs. (b) Decrease in fold expression of bcr/abl gene with DOX treatment, data represented as mean ± SEM ($n = 3$), $^*p < 0.05$, control vs (DOX+CUR) in solution and (DOX+CUR)-NPs.

based on the fact that CUR may help in retention of DOX inside the nucleus and may also inhibit the development of MDR leading to increased antiproliferative activity of the DOX in K562 cells. Because NP formulations of DOX and CUR are more active than the respective free drugs, it was anticipated that combining the two drugs in NPs would be beneficial. In this study, we have developed a sustained release formulation of (DOX+CUR) loaded PLGA-NPs. In general, all the NPs showed size below 250 nm with negative zeta potential (−13.8 mV). Both SEM and AFM studies confirmed the smooth and spherical surface of NPs. Moreover, TEM results demonstrated the uniform distribution of dual drug loaded NPs. FTIR results corroborated the stability of both the drugs in dual drug loaded NPs. To confirm that dual drug loaded NPs could be efficiently internalized by tumor cells, intracellular uptake of combination of drug in solution and in formulation by K562 cells were compared quantitatively by flow cytometry. Drug in solution enters through passive diffusion whereas NPs enter into the cells by endocytosis that results in higher uptake of NPs in comparison to drug in solution.[50] Besides this, expression of lower levels of MDR transporters can facilitate the intracellular drug sequestration leading to lower concentration of drug in solution than the NPs in K562 cells.[45,51] Cellular uptake study by fluorescence spectrophotometer revealed that cells treated with dual drug loaded NPs is showing more uptake of DOX compared to single DOX loaded NPs because the presence of CUR in dual drug loaded NPs inhibits further efflux of DOX by MDR leading to increased concentration of DOX in K562 cells. After separating the nucleus and cytoplasmic fraction, it was observed that dual drug loaded NPs helps in retention of higher amount of DOX in nucleus compared to all other formulations. This might be due to CUR in some way helping in retention of the DOX in the nucleus of K562 cells. Chen et al. have reported that DOX is effluxed out from the nucleus of the cells with increasing time of incubation due to formation of MVBs in K562 cells.[7,8] CUR might be inhibiting the formation of MVBs, or the presence of CUR in cytoplasm may be preventing the efflux of DOX from the nucleus of K562 cells. The mechanism of inhibition of DOX efflux from the nucleus of K562 cells by CUR is yet to be resolved. It was observed that the expression of MDR1 and BCL-2 significantly increases in 96 h after DOX treatment at the mRNA level leading to drug resistance. However, with CUR treatment the expression of MDR1 and BCL-2 gene decreases. Thus in dual drug loaded NPs, CUR inhibits the expression of MDR1 and BCL-2, leading to increasing efficacy of DOX both by retaining DOX in the nucleus and also by inhibiting the development of MDR in K562 cells. Figure 10a depicts that, with CUR treatment, the expression of bcr/abl gene decreases in 48 h of incubation. However, the dual drug loaded NPs showed comparatively higher inhibition of bcr/abl gene expression than all other different formulations.

From the above we can anticipate that the coadministration of DOX and CUR in NP formulation may help in enhanced efficacy of DOX by accumulating more DOX in the nucleus, leading to cytotoxicity in K562 cells. We have proved the above fact by several other *in vitro* studies using K562 cells. Cytotoxicity results depicted that, in dual drug loaded NPs, DOX is able to induce higher cytotoxicity even if at lower dose ($IC_{50} = 0.1\ \mu g/mL$) in K562 cells. Cell cycle analysis results depicted that the dual drug loaded NPs induced more G2/M arrest than all other formulations due to simultaneous G2/M arresting of both the drugs. Similarly, dual drug loaded NPs stimulated higher mitochondrial depolarization due to combined action of both the drugs concurrently. Both the drugs were able to trigger both intrinsic and extrinsic apoptotic pathways (Figure 9a−d) leading to further cell death. Thus, the combination of DOX and CUR in NP formulation can be utilized as a novel treatment regimen for CML.

In conclusion, our study demonstrates that coadministration of DOX and CUR in PLGA NPs can promote the cytotoxicity by both the drugs *in vitro* in leukemic cells. In this study, we have increased the therapeutic concentration of DOX inside the nucleus, by inhibition of nuclear efflux of DOX by CUR in K562 cells. Moreover, CUR helps in downregulation of both MDR1 and BCL-2 expression helping in stimulation of further cell death induced by DOX in K562 cells. Both the drugs combinedly induced a number of apoptotic pathways, leading to higher expression of a number of apoptotic proteins. RT-PCR results illustrate that the synergistic effect of both the drugs on apoptosis induction may help in downregulation of bcr/abl gene in K562 cells. In summary, DOX and CUR exhibited a synergistic inhibitory effect on the cell growth of K562. The synergistic growth inhibition was mediated through different mechanisms that involved the inhibition of p210bcr/abl. The synergistic effect is clinically important and may provide combinatorial strategies in cancer therapy.

AUTHOR INFORMATION

Corresponding Author

*Laboratory for Nanomedicine, Institute of Life Sciences, Nalco Square, Chandrasekharpur, Bhubaneswar, Orissa, India. Phone: 91-674-2302094. Fax: 91-674-2300728. E-mail: sanjeebsahoo2005@gmail.com.

ACKNOWLEDGMENT

R.M. would like to thank "Council of Scientific and Industrial Research", Government of India, for providing a senior research fellowship.

REFERENCES

(1) Czyz, M.; Jakubowska, J.; Sztiller-Sikorska, M. STI571/doxorubicin concentration-dependent switch for diverse caspase actions in CML cell line K562. *Biochem. Pharmacol.* **2008**, *75*, 1761–1773.

(2) Laroche-Clary, A.; Larrue, A.; Robert, J. Down-regulation of bcr-abl and bcl-x(L) expression in a leukemia cell line and its doxorubicin-resistant variant by topoisomerase II inhibitors. *Biochem. Pharmacol.* **2000**, *60*, 1823–1828.

(3) Wang, X.; Song, Y.; Ren, J.; Qu, X. Knocking-down cyclin A(2) by siRNA suppresses apoptosis and switches differentiation pathways in K562 cells upon administration with doxorubicin. *PLoS One* **2009**, *4*, e6665.

(4) Xiong, X. B.; Ma, Z.; Lai, R.; Lavasanifar, A. The therapeutic response to multifunctional polymeric nano-conjugates in the targeted cellular and subcellular delivery of doxorubicin. *Biomaterials* **2010**, *31*, 757–768.

(5) Fan, L.; Li, F.; Zhang, H.; Wang, Y.; Cheng, C.; Li, X.; Gu, C. H.; Yang, Q.; Wu, H.; Zhang, S. Co-delivery of PDTC and doxorubicin by multifunctional micellar nanoparticles to achieve active targeted drug delivery and overcome multidrug resistance. *Biomaterials* **2010**, *31*, 5634–5642.

(6) Rajagopal, A.; Simon, S. M. Subcellular localization and activity of multidrug resistance proteins. *Mol. Biol. Cell* **2003**, *14*, 3389–3399.

(7) Chen, V. Y.; Posada, M. M.; Blazer, L. L.; Zhao, T.; Rosania, G. R. The role of the VPS4A-exosome pathway in the intrinsic egress route of a DNA-binding anticancer drug. *Pharm. Res.* **2006**, *23*, 1687–1695.

(8) Chen, V. Y.; Posada, M. M.; Zhao, L.; Rosania, G. R. Rapid doxorubicin efflux from the nucleus of drug-resistant cancer cells following extracellular drug clearance. *Pharm. Res.* **2007**, *24*, 2156–2167.

(9) Zhang, K. Z.; Xu, J. H.; Huang, X. W.; Wu, L. X.; Su, Y.; Chen, Y. Z. Curcumin synergistically augments bcr/abl phosphorothioate antisense oligonucleotides to inhibit growth of chronic myelogenous leukemia cells. *Acta Pharmacol. Sin.* **2007**, *28*, 105–110.

(10) Hui, R. C.; Francis, R. E.; Guest, S. K.; Costa, J. R.; Gomes, A. R.; Myatt, S. S.; Brosens, J. J.; Lam, E. W. Doxorubicin activates FOXO3a to induce the expression of multidrug resistance gene ABCB1 (MDR1) in K562 leukemic cells. *Mol. Cancer Ther.* **2008**, *7*, 670–678.

(11) Pakunlu, R. I.; Cook, T. J.; Minko, T. Simultaneous modulation of multidrug resistance and antiapoptotic cellular defense by MDR1 and BCL-2 targeted antisense oligonucleotides enhances the anticancer efficacy of doxorubicin. *Pharm. Res.* **2003**, *20*, 351–359.

(12) Bill, M. A.; Bakan, C.; Benson, D. M., Jr.; Fuchs, J.; Young, G.; Lesinski, G. B. Curcumin induces proapoptotic effects against human melanoma cells and modulates the cellular response to immunotherapeutic cytokines. *Mol. Cancer Ther.* **2009**, *8*, 2726–2735.

(13) Sa, G.; Das, T. Anti cancer effects of curcumin: cycle of life and death. *Cell Div.* **2008**, *3*, 14.

(14) Reuter, S.; Charlet, J.; Juncker, T.; Teiten, M. H.; Dicato, M.; Diederich, M. Effect of curcumin on nuclear factor kappaB signaling pathways in human chronic myelogenous K562 leukemia cells. *Ann. N.Y. Acad. Sci.* **2009**, *1171*, 436–447.

(15) Anuchapreeda, S.; Leechanachai, P.; Smith, M. M.; Ambudkar, S. V.; Limtrakul, P. N. Modulation of P-glycoprotein expression and function by curcumin in multidrug-resistant human KB cells. *Biochem. Pharmacol.* **2002**, *64*, 573–582.

(16) Ganta, S.; Amiji, M. Coadministration of Paclitaxel and curcumin in nanoemulsion formulations to overcome multidrug resistance in tumor cells. *Mol. Pharmaceutics* **2009**, *6*, 928–939.

(17) Romiti, N.; Tongiani, R.; Cervelli, F.; Chieli, E. Effects of curcumin on P-glycoprotein in primary cultures of rat hepatocytes. *Life Sci.* **1998**, *62*, 2349–2358.

(18) Wu, L. X.; Xu, J. H.; Wu, G. H.; Chen, Y. Z. Inhibitory effect of curcumin on proliferation of K562 cells involves down-regulation of p210(bcr/abl) initiated Ras signal transduction pathway. *Acta Pharmacol. Sin.* **2003**, *24*, 1155–1160.

(19) Mohanty, C.; Acharya, S.; Mohanty, A. K.; Dilnawaz, F.; Sahoo, S. K. Curcumin-encapsulated MePEG/PCL diblock copolymeric micelles: a novel controlled delivery vehicle for cancer therapy. *Nanomedicine (London)* **2010**, *5*, 433–449.

(20) Mohanty, C.; Sahoo, S. K. The in vitro stability and in vivo pharmacokinetics of curcumin prepared as an aqueous nanoparticulate formulation. *Biomaterials* **2010**, *31*, 6597–6611.

(21) Jakubowska, J.; Stasiak, M.; Szulawska, A.; Bednarek, A.; Czyz, M. Combined effects of doxorubicin and STI571 on growth, differentiation and apoptosis of CML cell line K562. *Acta Biochim. Pol.* **2007**, *54*, 839–846.

(22) Mayer, L. D.; Janoff, A. S. Optimizing combination chemotherapy by controlling drug ratios. *Mol. Interventions* **2007**, *7*, 216–223.

(23) Lammers, T.; Subr, V.; Ulbrich, K.; Peschke, P.; Huber, P. E.; Hennink, W. E.; Storm, G. Simultaneous delivery of doxorubicin and gemcitabine to tumors in vivo using prototypic polymeric drug carriers. *Biomaterials* **2009**, *30*, 3466–3475.

(24) Sengupta, S.; Eavarone, D.; Capila, I.; Zhao, G.; Watson, N.; Kiziltepe, T.; Sasisekharan, R. Temporal targeting of tumour cells and neovasculature with a nanoscale delivery system. *Nature* **2005**, *436*, 568–572.

(25) Indap, M. A.; Radhika, S.; Motiwale, L.; Rao, K. V. Inhibitory effect of cinnamoyl compounds against human malignant cell line. *Indian J. Exp. Biol.* **2006**, *44*, 216–220.

(26) Kelkel, M.; Jacob, C.; Dicato, M.; Diederich, M. Potential of the dietary antioxidants resveratrol and curcumin in prevention and treatment of hematologic malignancies. *Molecules* **2010**, *15* (10), 7035–7074.

(27) Choi, B. H.; Kim, C. G.; Lim, Y.; Shin, S. Y.; Lee, Y. H. Curcumin down-regulates the multidrug-resistance mdr1b gene by inhibiting the PI3K/Akt/NF kappa B pathway. *Cancer Lett.* **2008**, *259*, 111–118.

(28) Das, M.; and Sahoo, S. K. Epithelial cell adhesion molecule targeted nutlin-3a loaded immunonanoparticles for cancer therapy. *Acta Biomater.* **2010**, *7*, 355−369

(29) Misra, R.; Sahoo, S. K. Intracellular trafficking of nuclear localization signal conjugated nanoparticles for cancer therapy. *Eur. J. Pharm. Sci.* **2010**, *39*, 152–163.

(30) Sahoo, S. K.; Ma, W.; Labhasetwar, V. Efficacy of transferrin-conjugated paclitaxel-loaded nanoparticles in a murine model of prostate cancer. *Int. J. Cancer* **2004**, *112*, 335–340.

(31) Shaikh, J.; Ankola, D. D.; Beniwal, V.; Singh, D.; Kumar, M. N. Nanoparticle encapsulation improves oral bioavailability of curcumin by at least 9-fold when compared to curcumin administered with piperine as absorption enhancer. *Eur. J. Pharm. Sci.* **2009**, *37*, 223–230.

(32) Acharya, S.; Dilnawaz, F.; Sahoo, S. K. Targeted epidermal growth factor receptor nanoparticle bioconjugates for breast cancer therapy. *Biomaterials* **2009**, *30*, 5737–5750.

(33) Chen, B.; Liang, Y.; Wu, W.; Cheng, J.; Xia, G.; Gao, F.; Ding, J.; Gao, C.; Shao, Z.; Li, G.; Chen, W.; Xu, W.; Sun, X.; Liu, L.; Li, X.; Wang, X. Synergistic effect of magnetic nanoparticles of Fe(3)O(4) with gambogic acid on apoptosis of K562 leukemia cells. *Int. J. Nanomed.* **2009**, *4*, 251–259.

(34) Dilnawaz, F.; Singh, A.; Mohanty, C.; Sahoo, S. K. Dual drug loaded superparamagnetic iron oxide nanoparticles for targeted cancer therapy. *Biomaterials* **2010**, *31*, 3694–3706.

(35) Misra, R.; Acharya, S.; Dilnawaz, F.; Sahoo, S. K. Sustained antibacterial activity of doxycycline-loaded poly(D,L-lactide-co-glycolide) and poly(epsilon-caprolactone) nanoparticles. *Nanomedicine (London)* **2009**, *4*, 519–530.

(36) Vandana, M.; Sahoo, S. K. Long circulation and cytotoxicity of PEGylated gemcitabine and its potential for the treatment of pancreatic cancer. *Biomaterials* **2010**, *31*, 9340–9356.

(37) Fang, G.; Kim, C. N.; Perkins, C. L.; Ramadevi, N.; Winton, E.; Wittmann, S.; Bhalla, K. N. CGP57148B (STI-571) induces differentiation and apoptosis and sensitizes Bcr-Abl-positive human leukemia cells to apoptosis due to antileukemic drugs. *Blood* **2000**, *96*, 2246–2253.

(38) Sanchez, Y.; Simon, G. P.; Calvino, E.; de Blas, E.; Aller, P. Curcumin stimulates reactive oxygen species production and potentiates apoptosis induction by the antitumor drugs arsenic trioxide and lonidamine in human myeloid leukemia cell lines. *J. Pharmacol. Exp. Ther.* **2010**, *335*, 114–123.

(39) Toffoli, G.; Viel, A.; Bevilacqua, C.; Maestro, R.; Tumiotto, L.; Boiocchi, M. In K562 leukemia cells treated with doxorubicin and hemin, a decrease in c-myc mRNA expression correlates with loss of self-renewal capability but not with erythroid differentiation. *Leuk. Res.* **1989**, *13*, 279–287.

(40) Gao, M.; Fan, S.; Goldberg, I. D.; Laterra, J.; Kitsis, R. N.; Rosen, E. M. Hepatocyte growth factor/scatter factor blocks the mitochondrial pathway of apoptosis signaling in breast cancer cells. *J. Biol. Chem.* **2001**, *276*, 47257–47265.

(41) Jakubowska, J.; Wasowska-Lukawska, M.; Czyz, M. STI571 and morpholine derivative of doxorubicin collaborate in inhibition of K562 cell proliferation by inducing differentiation and mitochondrial pathway of apoptosis. *Eur. J. Pharmacol.* **2008**, *596*, 41–49.

(42) Cilloni, D.; Saglio, G. CML: a model for targeted therapy. *Best Pract. Res. Clin. Haematol.* **2009**, *22*, 285–294.

(43) Salesse, S.; Verfaillie, C. M. BCR/ABL: from molecular mechanisms of leukemia induction to treatment of chronic myelogenous leukemia. *Oncogene* **2002**, *21*, 8547–8559.

(44) Gong, Y.; Duvvuri, M.; Krise, J. P. Separate roles for the Golgi apparatus and lysosomes in the sequestration of drugs in the multidrug-resistant human leukemic cell line HL-60. *J. Biol. Chem.* **2003**, *278*, 50234–50239.

(45) Noskova, V.; Dzubak, P.; Kuzmina, G.; Ludkova, A.; Stehlik, D.; Trojanec, R.; Janostakova, A.; Korinkova, G.; Mihal, V.; Hajduch, M. In vitro chemoresistance profile and expression/function of MDR associated proteins in resistant cell lines derived from CCRF-CEM, K562, A549 and MDA MB 231 parental cells. *Neoplasma* **2002**, *49*, 418–425.

(46) Bedi, A.; Barber, J. P.; Bedi, G. C.; el-Deiry, W. S.; Sidransky, D.; Vala, M. S.; Akhtar, A. J.; Hilton, J.; Jones, R. J. BCR-ABL-mediated inhibition of apoptosis with delay of G2/M transition after DNA damage: a mechanism of resistance to multiple anticancer agents. *Blood* **1995**, *86*, 1148–1158.

(47) Hochhaus, A.; Reiter, A.; Skladny, H.; Melo, J. V.; Sick, C.; Berger, U.; Guo, J. Q.; Arlinghaus, R. B.; Hehlmann, R.; Goldman, J. M.; Cross, N. C. A novel BCR-ABL fusion gene (e6a2) in a patient with Philadelphia chromosome-negative chronic myelogenous leukemia. *Blood* **1996**, *88*, 2236–2240.

(48) Prasad, S.; Phromnoi, K.; Yadav, V. R.; Chaturvedi, M. M.; Aggarwal, B. B. Targeting inflammatory pathways by flavonoids for prevention and treatment of cancer. *Planta Med.* **2010**, *76*, 1044–1063.

(49) Park, J.; Ayyappan, V.; Bae, E. K.; Lee, C.; Kim, B. S.; Kim, B. K.; Lee, Y. Y.; Ahn, K. S.; Yoon, S. S. Curcumin in combination with bortezomib synergistically induced apoptosis in human multiple myeloma U266 cells. *Mol. Oncol.* **2008**, *2*, 317–326.

(50) Sahoo, S. K.; Labhasetwar, V. Enhanced antiproliferative activity of transferrin-conjugated paclitaxel-loaded nanoparticles is mediated via sustained intracellular drug retention. *Mol. Pharmaceutics* **2005**, *2*, 373–383.

(51) Ferrao, P.; Sincock, P.; Cole, S.; Ashman, L. Intracellular P-gp contributes to functional drug efflux and resistance in acute myeloid leukaemia. *Leuk. Res.* **2001**, *25*, 395–405.